Report

Current Biology

# Exceptionally preserved beetles in a Triassic coprolite of putative dinosauriform origin

## Highlights

- The beetle *Triamyxa coprolithica* is described from a Triassic coprolite
- It represents the only member of the extinct myxophagan family Triamyxidae
- The coprolite was likely produced by the dinosauriform *Silesaurus opolensis*
- The beetle fossils parallel younger amber inclusions in preservation quality

## Authors

Martin Qvarnström, Martin Fikáček, Joel Vikberg Wernström, ..., Emmanuel Arriaga-Varela, Per E. Ahlberg, Grzegorz Niedźwiedzki

## Correspondence

martin.qvarnstrom@ebc.uu.se (M.Q.), mfikacek@gmail.com (M.F.), grzegorz.niedzwiedzki@ebc.uu.se (G.N.)

## In brief

Qvarnström et al. use synchrotron microtomography to describe 3D-preserved beetle fossils from a Triassic coprolite. Most specimens belong to the new beetle *Triamyxa coprolithica*, which represents the only member of the extinct myxophagan family Triamyxidae. The fossil dropping was likely produced by the dinosauriform *Silesaurus opolensis*.

Qvarnström et al., 2021, Current Biology *31*, 1–8
August 9, 2021 
https://doi.org/10.1016/j.cub.2021.05.015

CellPress

Current Biology

CellPress
OPEN ACCESS

Report

# Exceptionally preserved beetles in a Triassic coprolite of putative dinosauriform origin

Martin Qvarnström,[1,8,*] Martin Fikácek,[2,3,4,*] Joel Vikberg Wernström,[1] Sigrid Huld,[5] Rolf G. Beutel,[6] Emmanuel Arriaga-Varela,[7] Per E. Ahlberg,[1] and Grzegorz Niedzwiedzki[1,*]

[1]Department of Organismal Biology, Evolutionary Biology Centre, Uppsala University, Norbyvägen 18A, 752 36 Uppsala, Sweden
[2]Department of Biological Sciences, National Sun Yat-sen University, no. 70, Lienhai Road, Kaohsiung 80424, Taiwan
[3]Department of Entomology, National Museum, Praha 9, Czech Republic
[4]Department of Zoology, Faculty of Science, Charles University, Praha 2, Czech Republic
[5]Geocentrum, Uppsala University, Villavägen 16, 752 36 Uppsala, Sweden
[6]Institut für Zoologie und Evolutionsforschung, Friedrich-Schiller-Universität Jena, Jena, Germany
[7]Centro de Estudios en Zoología, CUCBA, Universidad de Guadalajara, Zapopan, Mexico
[8]Lead contact
*Correspondence: martin.qvarnstrom@ebc.uu.se (M.Q.), mfikacek@gmail.com (M.F.), grzegorz.niedzwiedzki@ebc.uu.se (G.N.)
https://doi.org/10.1016/j.cub.2021.05.015

## SUMMARY

The Triassic was a crucial period for the early evolution and diversification of insects, including Coleoptera[1–3]—the most diverse order of organisms on Earth. The study of Triassic beetles, however, relies almost exclusively on flattened fossils with limited character preservation. Using synchrotron microtomography, we investigated a fragmentary Upper Triassic coprolite, which contains a rich record of 3D-preserved minute beetle remains of *Triamyxa coprolithica* gen. et sp. nov. Some specimens are nearly complete, preserving delicate structures of the legs and antennae. Most of them are congruent morphologically, implying that they are conspecific. Phylogenetic analyses suggest that *T. coprolithica* is a member of Myxophaga, a small suborder of beetles with a sparse fossil record, and that it represents the only member of the extinct family Triamyxidae fam. nov. Our findings highlight that coprolites can contain insect remains, which are almost as well preserved as in amber. They are thus an important source of information for exploring insect evolution before the Cretaceous-Neogene "amber time window." Treated as food residues, insect remains preserved in coprolites also have important implications for the paleoecology of insectivores, in this case, likely the dinosauriform *Silesaurus opolensis.*

## RESULTS

Beetles (Coleoptera) are an extremely diverse and abundant order of insects, occurring in almost all terrestrial or freshwater habitats across the globe. Molecular clocks suggest that the group may have originated in the Carboniferous.[1] The definite fossil record dates back to the Permian,[4–6] and modern lineages started to diversify in the Triassic.[1–3] Most abundance and diversity data on fossil beetles derive from fine-grained lacustrine deposits and amber. Amber yields exceptional 3D-preserved beetles but was only formed when enough suitable resin-producing trees were present. Although such trees have existed since the Carboniferous, the first large masses of resin that became preserved as amber were produced in the Early Cretaceous (approximately 130 Ma).[7] Only few arthropods, but no beetles, have been described from amber older than that,[8] and consequently, the fossil record of beetles prior to the Early Cretaceous is entirely derived from non-amber deposits.[9]

Other types of 3D preservation of insects include specimens preserved as mineralized replicas (e.g., silicified, phosphatized, or pyritized), as voids, in chert, or within vertebrate coprolites (fossil excrement). In recent years, it has become evident that coprolites may act as microenvironments in which organic inclusions can be better preserved than in the host rock.[10–12] Coprolites can contain inclusions that otherwise are rarely preserved as fossils (e.g., soft tissues), and these are preserved three-dimensionally, even when derived from highly compacted host sediments. The inclusions from coprolites can be used to infer character states of extinct animals,[13,14] and they also carry important information on diets, digestive strategies, and trophic structures of past ecosystems.[11,15–21]

A cast of an insect head has previously been described from a Triassic coprolite from Australia.[22] Here, we describe 3D-preserved beetle remains, including complete specimens, from the late Carnian beds exposed at Krasiejów locality in Poland. Isolated beetle remains have previously been described from Krasiejów in clay-rich sediments[23] and in coprolites tentatively attributed to the dinosauriform *Silesaurus opolensis*.[19] The coprolite described here was scanned using phase-contrast propagation synchrotron microtomography, a technique shown as highly suitable for reconstructing coprolite inclusions.[24]

### The coprolite

Specimen ZPAL AbIII/3520 is 17 mm long and cylindrical, with a diameter of 21 mm. Its shape, the two broken ends, and


**Figure 1. Contents of coprolite fragment ZPAL AbIII/3520**

(A) The coprolite rendered semi-transparent with inclusions, such as beetle remains and fibrous networks, representing fungal colonies or algae visible. Top corner: silhouette of *Silesaurus opolensis*, the most probable coprolite producer.

(B–D) The holotype specimen of *Triamyxa coprolithica* in ventral (B), lateral (C), and dorsal (D) views.

(E and F) The second complete specimen in ventral (E) and anterior (F) views. Individual ventrites are indicated by roman numerals.

(G) *Triamyxa coprolithica* preserved in various degrees of disarticulation.

(H) An isolated head and two elytra that do not belong to *Triamyxa coprolithica* but to slightly larger beetles that were also ingested by the coprolite producer.

(I) Examples of individual remains of *Triamyxa coprolithica* (meso- and metaventrite, head, head attached to pronotum, and three pronota).

(J) Two of numerous elytra of similar size and morphology attributed to *T. coprolithica*.

(K) Fibrous structures interpreted as fungi or algae.

(L) A possible decomposed wood fragment.

Color coding: blue, eyes; purple, antennae; light purple, legs. Abbreviations: abd, abdomen; ant, antenna; cox, coxa; ey, eye; fem, femur; hd, head; lgs, legs; pp, propleuron; thx, thorax; tib, tibia; troch, trochanter; trs, tarsi; ventr, ventrites. See also Figure S1.

comparisons with other coprolites in the collection suggest that it represents a small fragment of an elongated specimen (Figures 1 and S1A). It contains near-complete fossils as well as isolated heads, pronota, elytra, and other sclerites, which all are embedded in the phosphate-rich coprolite matrix. Visualization was accomplished using 3D reconstructions based on synchrotron scans (Figure 1). Most beetle inclusions (Figures 1G, 1I, and 1J) are very similar in size and share

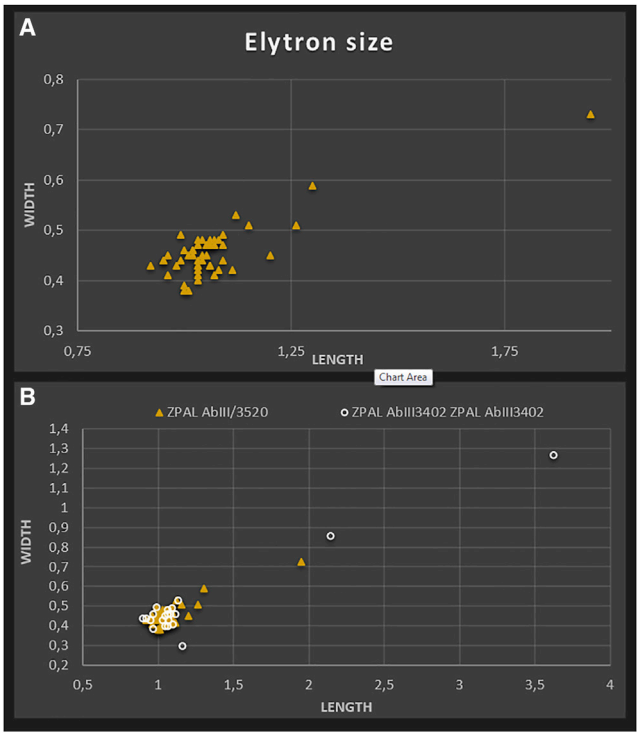


**Figure 2. Scatterplots showing the size distribution of the elytra**
(A) Elytra from ZPAL AbIII/3520.
(B) The elytra from ZPAL AbIII/3520 compared to those of ZPAL AbIII/3402 (see Discussion and Qvarnström et al.[19]). Note that both coprolites contain many similar-sized elytra attributed to *Triamyxa coprolithica* but also a few larger ones.

morphological details and can thus be assigned to the same species. Only three elytra and a few other disarticulated beetle remains are not conspecific with the other specimens and apparently belonged to larger species (Figures 1H, 2, and S1). The coprolite matrix is heterogeneous and contains abundant minuscule inclusions, many likely representing unidentifiable and very disarticulated or digested remains of beetles and other insects. In addition, several "colonies" of small fibrous networks are visible in the coprolite, which likely represent fossilized fungi or algae (Figure 1K). Some inclusions lack sufficient morphological features to be identified, including material possibly representing a decomposed wood fragment (Figure 1L).

## Phylogenetic position of the fossil beetle

The unconstrained analysis of the Coleoptera dataset suggests a placement of the beetle in the polyphagan superfamily Staphylinoidea (posterior probability pp = 0.67), with weakly supported alternative placements in families Ptiliidae, Staphylinidae (Scaphidiinae), or Hydrophilidae (Figure S2). However, all these families are characterized by a number of synapomorphies absent in the fossil beetle and can be reliably excluded. Moreover, the superimposition of isolated prothoraces on more complete specimens (Figures 3R–3T) revealed the presence of a large exposed propleuron. An exposed propleuron is present in Archostemata, Myxophaga, and Adephaga but is consistently absent in Polyphaga (Figures 3I–3Q). Thus, its presence clearly excludes the placement of the fossil in this megadiverse suborder. Accordingly, the Coleoptera analysis in which the fossil beetle was constrained from being placed in Polyphaga supported its placement in the suborder Myxophaga (pp = 0.95; Figures 3A and 3B). A position within this small group is corroborated by several characters shared with other myxophagan taxa (see Discussion). Bayesian analyses of Coleoptera and Myxophaga datasets with constrained molecular topology suggest a sister group relationship with the entire modern Myxophaga (Figures 3B and 3F). Maximum parsimony analyses place it either in an unresolved basal polytomy (analyses with constrained molecular topology; Figure 3G) or as sister to Hydroscaphidae (unconstrained analyses; Figure 3H). In summary, our analyses reveal that the fossil beetle represents an extinct lineage within the small suborder Myxophaga, with unclear relationships to modern subgroups. The morphological comparison with extant families corroborates these results and confirms the fossil as a species of an extinct lineage of the suborder. The four extant families of Myxophaga comprise about 120 species. They are all of small size and typically found in aquatic to moist environments associated with algal mats (Figure S1).

## Systematics

Order Coleoptera
Suborder Myxophaga

### Family Triamyxidae fam. nov.

#### *Type genus*

*Triamyxa* gen. nov.

#### *Differential diagnosis*

Characters of the new family are put in contrast to [×] other myxophagan families: dorsal body surface without tubercles or ridges (×Lepiceridae); eyes strongly protruding (×Sphaeriusidae, most Hydroscaphidae); head anterior of eyes prolonged and distinctly narrowing (×Hydroscaphidae, Sphaeriusidae); antennal bases exposed dorsally between eyes (×Hydroscaphidae, Lepiceridae); antennal scapus and pedicel distinctly separated from each other (×Torridincolidae, Lepiceridae), exposed in dorsal view (×Lepiceridae, modern Hydroscaphidae); terminal maxillary palpomere long, longer than penultimate (×Hydroscaphidae, Sphaeriusidae); mentum large, narrowing anteriad (×modern Hydroscaphidae); prosternum long, with very short prosternal process (×Hydroscaphidae, Lepiceridae); propleuron wide, without posterior projection (×all modern families); mesoventrite only slightly shorter than metaventrite (×Hydroscaphidae, Sphaeriusidae, Torridincolidae); mesoventrite with wide subpentagonal elevation (×modern Hydroscaphidae, Torridincolidae); elytra only slightly shortened, exposing 1 to 2 terminal abdominal tergites (×all modern families), truncated posteriorly (×Sphaeriusidae, Torridincolidae, Lepiceridae); metanepisternum moderately wide anteriorly (×Sphaeriusidae, Torridincolidae, Lepiceridae); metacoxal plates present, narrow (×Sphaeriusidae, Torridincolidae, Lepiceridae); abdomen with 5 to 6 exposed ventrites (Figure 4; ×Sphaeriusidae, some Torridincolidae); all abdominal segments with separate

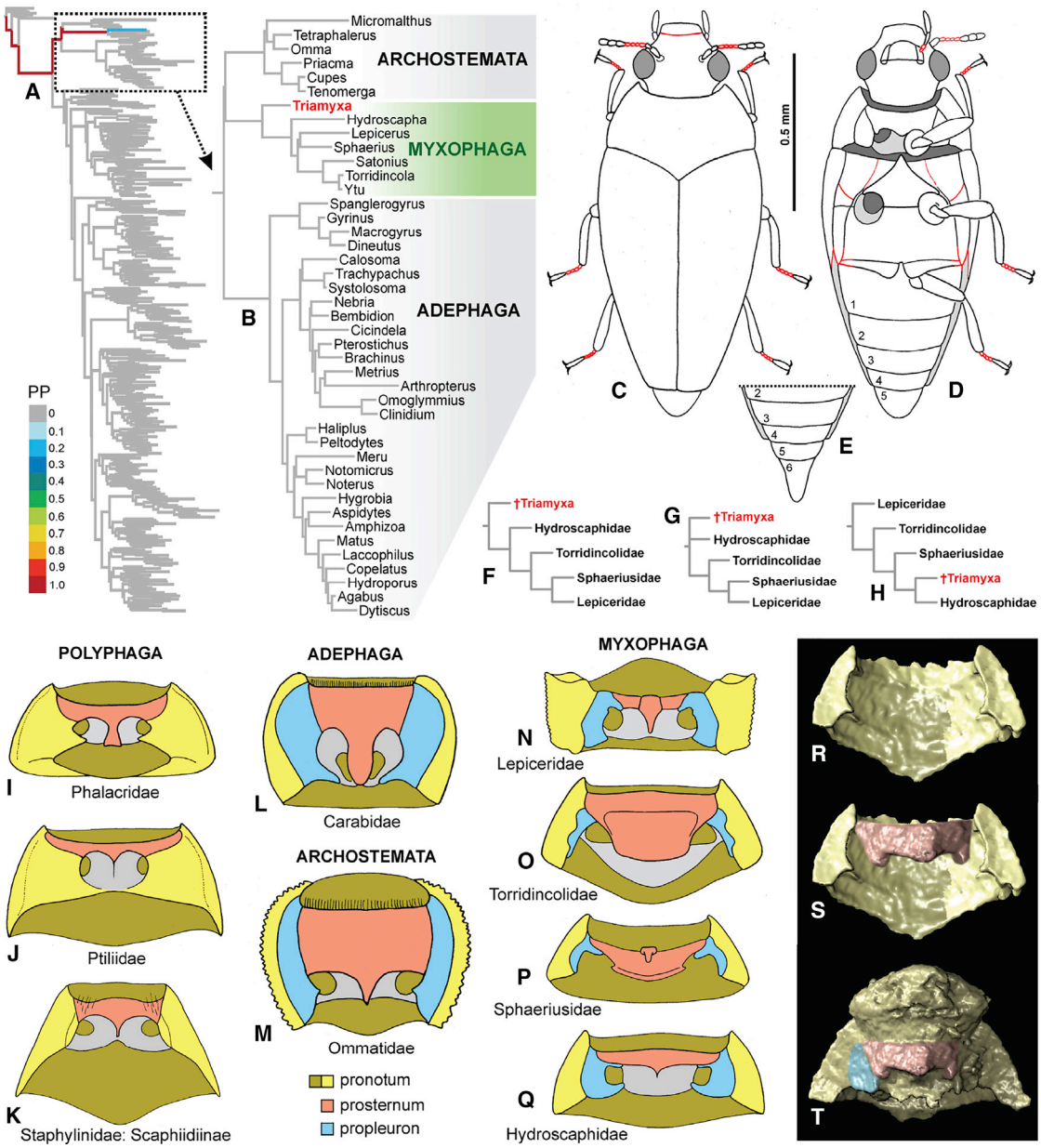


**Figure 3. Phylogenetic position and morphology of *Triamyxa coprolithica***

(A and B) Results of Bayesian analysis of Coleoptera dataset, with fossil position in Polyphaga excluded following the prothorax morphology: (A) complete beetle tree with color-coded posterior probabilities (PPs) of *Triamyxa* position; (B) maximum credibility tree with Polyphaga not shown.

(C–E) Reconstruction of *Triamyxa* morphology: (C) dorsal view; (D) ventral view of a specimen with 5-segmented abdomen; (E) specimen with exposed 6$^{th}$ abdominal ventrite (see Figure 4 for comparison of all specimens).

(F–H) Alternative positions of *Triamyxa* revealed by Myxophaga analyses: (F) Bayesian, molecular topology constrained; (G) maximum parsimony, molecular topology constrained; (H) maximum parsimony, topology unconstrained.

(I–Q) Comparative morphology of the prothorax in ventral view: (I) *Olibrus*; (J) *Acrotrichis*; (K) *Scaphidium*; (L) *Nebria*; (M) *Beutelius*; (N) *Lepicerus*; (O) *Satonius*; (P) *Sphaerius*; (Q) *Hydroscapha*.

(R–T) Prothoracic morphology of *Triamyxa* revealed by superimposition of disarticulated remains: (R) isolated pronotum; (S) isolated pronotum with superimposed prosternum from another specimen; (T) final reconstruction with the position of propleuron.

See also Figures S2 and S3.

tergite and sternite (×Hydroscaphidae). For more details, see Table S1. From its habitus, Triamyxidae is similar to Hydroscaphidae but differs from this family in a series of characters listed above, most notably the lack of fused tergites and sternites of abdominal segments III–VI. This abdominal configuration, a very uncommon shared derived feature and synapomorphy of extant Hydroscaphidae and the Triassic *Leehermania*, is clearly absent from *Triamyxa*, where tergites and

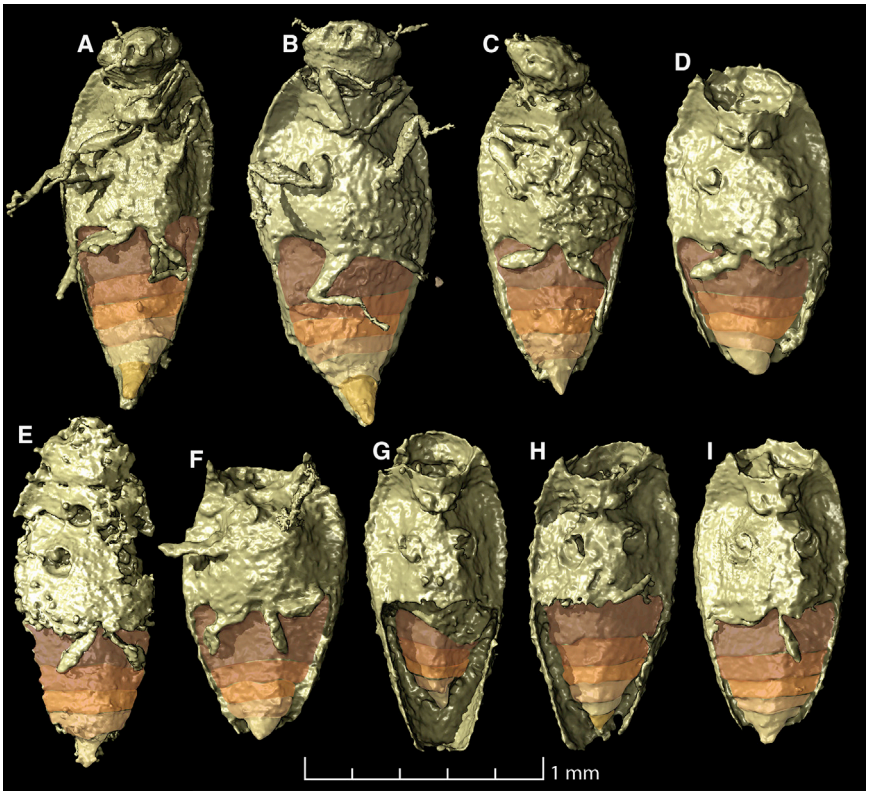


**Figure 4. Ventral view of near-complete specimens of *Triamyxa coprolothica* gen. and sp. nov. showing the variation in the number of abdominal ventrites**

The specimens are color coded based on the most probable abdominal segmentation, which is either five (C–G and I) or six (A, B, and H). However, the preservation of some specimens (C, E, G, and I) makes it difficult to tell whether they have five or actually six ventrites.

sternites of all abdominal segments are distinctly separated (Figure S1).

### *Triamyxa coprolithica* gen. et sp. nov.

#### Type species of the genus

*T. coprolithica* sp. nov.

#### Type material

Holotype: complete specimen (Figures 1B–1D) preserved in coprolite ZPAL AbIII/3520, stored at the Institute of Paleobiology, Polish Academy of Sciences (Warsaw). Paratypes: one complete and 13 partly to totally disarticulated specimens in the same coprolite (Figures 1E–1G and 1I). The publication is registered in ZooBank: http://zoobank.org/urn:lsid:zoobank.org:pub:6FB8E4B4-51C6-493C-A1E6-1829B9258993, to describe the new species as a valid taxon.

#### Type locality and horizon

Krasiejów clay pit, near Ozimek, Upper Silesia, Poland. The material from the upper bonebed, part of the Keuper succession from Silesia, can be correlated with the Drawno Beds. Biostratigraphic data support a late Carnian age of the Krasiejów biota.

#### Diagnosis

Body length 1.4–1.7 mm, elytra 0.9–1.3 mm long and 0.4–0.5 mm wide. Body elongate navicular (Figure 1F). Diagnostic characters as for the family. A detailed description of the new species is provided in STAR Methods.

## DISCUSSION

It can be challenging to reliably assign fossil insects even to higher taxonomic ranks, as important characters can be rendered ambiguous by fossilization processes and thus become prone to misinterpretation. For example, the supposed "oldest beetle"[25] was removed from the order Coleoptera,[26] and the phylogenetic position of the Triassic *Leehermania* was shifted from polyphagan rove beetles (Staphylinidae) to the small suborder Myxophaga.[27] The insect fossils studied herein bear all synapomorphies of modern beetles and thus undoubtedly belong to Coleoptera. Their exceptional 3D preservation, revealed by synchrotron microtomography, allowed us to reconstruct the morphology of this tiny beetle in sufficient detail to analyze its precise phylogenetic placement. The exposed propleuron of *Triamyxa* is a plesiomorphic character within beetles, which reliably excludes it from Polyphaga, where it is completely internalized, without a single case of reversal in any of the circa 150 families. The firmly connected meso- and metaventrite of *Triamyxa* is an apomorphy shared with Polyphaga and Myxophaga. This condition is unknown in Adephaga and Archostemata.[28] Derived features shared with Myxophaga are the widely separated mesocoxae, a pentagonal mesoventral elevation, and the presence of coxal plates. In addition, a long terminal tarsomere and small body size are consistent with an assignment to this suborder. The boat-shaped body, the truncated elytra, and a sixth exposed abdominal ventrite in some specimens (either facultatively or in males only) suggest phylogenetic affinities with Hydroscaphidae. Parallel evolution of these characters cannot be excluded with certainty, and our analyses leave the precise position of *Triamyxa* open. However, the character analyses unambiguously show that *Triamyxa* is not nested within Hydroscaphidae or any other myxophagan family. Therefore, it represents a hitherto unknown extinct offshoot (and the first representative of an extinct family) of the small suborder.

Myxophaga, placed as sister to Polyphaga based on morphology[28] and as closest relative of the "archaic" Archostemata based on transcriptomes,[1] apparently plays a pivotal role in beetle phylogenetics. The fossil record for this small group was minimal to absent for a long time but was improved with the discovery of Burmese amber inclusions (e.g., Jałoszynski et al.[29]) and the re-interpretation of *Leehermania*.[27] The discovery of *Triamyxa* further improves the knowledge of the evolutionary history of the suborder and suggests (together with findings of fossil representatives of three out of four extant myxophagan families

and *Leehermania*) that the Mesozoic taxonomic diversity of Myxophaga was higher than today and later trimmed by extinction. However, *Triamyxa* is morphologically similar to modern representatives of the suborder, implying that the wide gap in morphology between Myxophaga and Archostemata likely evolved before the Triassic. Except for Lepiceridae, *Triamyxa* closely resembles modern myxophagans by its general habitus, small body size, and concentration in large numbers. This suggests that *Triamyxa*, similar to extant myxophagan beetles, had a lifestyle closely associated with water and probably algal mats. Consequently, members of Myxophaga had colonized aquatic habitats at an early stage of beetle evolution, in parallel to unrelated lineages of Adephaga[6] and Polyphaga.[1]

Fungal and bacterial activities likely influenced the preservation of the beetles; some surfaces are uneven, whereas others are smooth with sharply defined edges, and a few specimens are affected by intensive secondary mineralization. This underlines that the preservation of coprolites is strongly influenced by microbial processes, which is also supported by remains of bacterial pseudomorphs commonly found in coprolite matrices.[12,30,31] That the beetles are found in various degrees of disarticulation clearly shows that they were ingested rather than having colonized the feces for feeding or laying eggs. Besides this, no surface traces or burrows were found in association to the body fossils (cf. Chin and Gill).[32] The minute size and well-preserved state of the beetles suggest that they may have been accidentally ingested with algae rather than targeted prey.

The small elytra of *Triamyxa coprolithica* found in ZPAL AbIII/3520 match, in terms of size and morphology, those earlier described from coprolites attributed to *Silesaurus opolensis* (Figure 4; Qvarnström et al.[19]). Similar elytra appear also in other coprolites from Krasiejów but are typically scarce and heavily outnumbered by other inclusions (commonly fish scales), which are more likely remains of the actual targeted food source (unpublished data). The only coprolite with a comparable amount of beetle remains as found here is ZPAL AbIII/3402.[19] It contains small elytra of *Triamyxa* as well as isolated remains of larger beetles. In a similar manner, the coprolite described here contains a head and a few elytra of larger coleopteran species (Figure 1H). Consequently, the only two coprolites from Krasiejów with high concentrations of small beetle body parts also contain isolated fragments of larger species. The producer of these coprolites ingested more beetles in terms of numbers and species diversity than other animals from Krasiejów, suggesting that insects were a regular food source.

The sheer number of *Triamyxa* specimens in the coprolites suggests that it was very abundant where the coprolite producer was foraging. Modern myxophagan species often occur in large numbers in association with green algae in aquatic or semi-aquatic habitats (Figures S1D and S1E),[33] and a similar lifestyle may be expected for *Triamyxa*. Given its small size and sclerotized body surface, *Triamyxa* obviously had a better chance to survive digestion than other insects (without becoming mechanically disintegrated, regurgitated, or completely digested). Even though beetles were found in large numbers, it is conceivable that the coprolite producer, likely the dinosauriform *Silesaurus opolensis* (based on the argumentation of Qvarnström et al.[19]), was not strictly insectivorous. It may have ingested soft-bodied organisms that never ended up in the excrement or did so but in a completely unrecognizable form.

This study further highlights the potential of coprolites, and other phosphatic bromalites,[34] to function as microenvironments for exceptional preservation of organic inclusions. Coprolites from insectivores can be of great use to study extinct beetles because (1) they can be heavily concentrated in the droppings, (2) the beetles are often well preserved, and (3) they potentially originate from environments with poor preservation potential. To end up in a recognizable form, however, the insects must survive the digestive system of the producer. Small beetles with a strongly sclerotized body surface apparently have a much better chance to appear in full articulation than soft-bodied insects or other animals. The discovery of *Triamyxa*—the first insect species described from a vertebrate coprolite—demonstrates that the Triassic coprolite insects parallel younger amber inclusions in quality of preservation. Coprolites may thus be valuable for studying insect evolution, especially prior to the large-scale formation of tree resin in the Early Cretaceous. In addition, insect remains from insectivore coprolites will expand our knowledge of their paleoecology and cast new light on food web structures in past ecosystems.

## STAR★METHODS

Detailed methods are provided in the online version of this paper and include the following:

- KEY RESOURCES TABLE
- RESOURCE AVAILABILITY
  - Lead contact
  - Materials availability
  - Data and code availability
- EXPERIMENTAL MODEL AND SUBJECT DETAILS
- METHOD DETAILS
  - Synchrotron microtomography
  - Examined material and character reconstruction
  - Phylogenetic analyses
  - Characters coded for Coleoptera analysis
  - Characters coded for Myxophaga dataset
  - Results of phylogenetic analyses (see also Figures S2 and S3)
  - Description of Triamyxa coprolithica gen. & sp. nov
  - The locality
- QUANTIFICATION AND STATISTICAL ANALYSIS
- ADDITIONAL RESOURCES

## SUPPLEMENTAL INFORMATION

Supplemental information can be found online at https://doi.org/10.1016/j.cub.2021.05.015.

## ACKNOWLEDGMENTS

The coprolite was scanned at the European Synchrotron Radiation Facility (ESRF) in Grenoble as a part of proposal ES145. Many thanks to Paul Tafforeau for help during the scan session and for reconstructing the scan data. We would also like to thank Paula Dentzien-Dias for comments on an earlier draft of the paper and three anonymous reviewers for comments that improved the final version of the paper. M.F. was funded by the Ministry of Culture of the Czech Republic (DKRVO 2019–2023/5.I.c, National Museum, 00023272).

E.A.-V. is funded by a postdoctoral grant by CONACYT, Mexico. P.E.A. is supported by a Wallenberg Scholarship from the Knut & Alice Wallenberg Foundation. M.Q. is funded by a scholarship from E. and K.G. Lennanders Foundation.

## AUTHOR CONTRIBUTIONS

M.Q., P.E.A., and G.N. conceived the project. M.Q. and G.N. performed synchrotron scanning. S.H., J.V.W., and M.Q. segmented the scan data. M.F., R.G.B., and E.A.-V. examined the morphology and coded morphological characters. M.F. ran phylogenetic analyses. All authors wrote and accepted the final version of the manuscript.

## DECLARATION OF INTERESTS

The authors declare no competing interests.

Received: February 25, 2021
Revised: April 16, 2021
Accepted: May 10, 2021
Published: June 30, 2021

## REFERENCES

1. McKenna, D.D., Shin, S., Ahrens, D., Balke, M., Beza-Beza, C., Clarke, D.J., Donath, A., Escalona, H.E., Friedrich, F., Letsch, H., et al. (2019). The evolution and genomic basis of beetle diversity. Proc. Natl. Acad. Sci. USA *116*, 24729–24737.
2. Toussaint, E.F.A., Seidel, M., Arriaga-Varela, E., Hájek, J., Král, D., Sekerka, L., Short, A.E.Z., and Fikácek, M. (2017). The peril of dating beetles. Syst. Entomol. *42*, 1–10.
3. Zhang, S.-Q., Che, L.-H., Li, Y., Dan Liang, Pang, H., Ślipinski, A., and Zhang, P. (2018). Evolutionary history of Coleoptera revealed by extensive sampling of genes and species. Nat. Commun. *9*, 205.
4. Kirejtshuk, A.G., Poschmann, M., Prokop, J., Garrouste, R., and Nel, A. (2014). Evolution of the elytral venation and structural adaptations in the oldest Palaeozoic beetles (Insecta: Coleoptera: Tshekardocoleidae). J. Syst. Palaeontology *12*, 575–600.
5. Yan, E.V., Lawrence, J.F., Beattie, R., and Beutel, R.G. (2018). At the dawn of the great rise: †*Ponomarenkia belmonthensis* (Insecta: Coleoptera), a remarkable new Late Permian beetle from the Southern Hemisphere. J. Syst. Palaeontology *16*, 611–619.
6. Yan, E.V., Beutel, R.G., and Lawrence, J.F. (2018). Whirling in the late Permian: ancestral Gyrinidae show early radiation of beetles before Permian-Triassic mass extinction. BMC Evol. Biol. *18*, 33.
7. Poinar, G.O., Jr. (1992). Life in Amber (Stanford University).
8. Schmidt, A.R., Jancke, S., Lindquist, E.E., Ragazzi, E., Roghi, G., Nascimbene, P.C., Schmidt, K., Wappler, T., and Grimaldi, D.A. (2012). Arthropods in amber from the Triassic Period. Proc. Natl. Acad. Sci. USA *109*, 14796–14801.
9. Smith, D.M., and Marcot, J.D. (2015). The fossil record and macroevolutionary history of the beetles. Proc. R. Soc. B *282*, 20150060.
10. Seilacher, A., Marshall, C., Skinner, H.C.W., and Tsuihiji, T. (2001). A fresh look at sideritic "coprolites". Paleobiology *27*, 7–13.
11. Chin, K., Eberth, D.A., Schweitzer, M.H., Rando, T.A., Sloboda, W.J., and Horner, J.R. (2003). Remarkable preservation of undigested muscle tissue within a Late Cretaceous tyrannosaurid coprolite from Alberta, Canada. Palaios *18*, 286–294.
12. Qvarnström, M., Niedzwiedzki, G., and Žigaitė, Ž. (2016). Vertebrate coprolites (fossil faeces): an underexplored *Konservat-Lagerstätte*. Earth Sci. Rev. *162*, 44–57.
13. Meng, J., and Wyss, A.R. (1997). Multituberculate and other mammal hair recovered from Palaeogene excreta. Nature *385*, 712–714.
14. Bajdek, P., Qvarnström, M., Owocki, K., Sulej, T., Sennikov, A.G., Golubev, V.K., and Niedzwiedzki, G. (2016). Microbiota and food residues including possible evidence of pre-mammalian hair in Upper Permian coprolites from Russia. Lethaia *49*, 455–477.
15. Hunt, A.P., Chin, K., and Lockley, M.G. (1994). The paleobiology of vertebrate coprolites. In The Paleobiology of Trace Fossils, S.K. Donovan, ed. (John Wiley), pp. 221–240.
16. Niedzwiedzki, G., Bajdek, P., Qvarnström, M., Sulej, T., Sennikov, A.G., and Golubev, V.K. (2016). Reduction of vertebrate coprolite diversity associated with the end-Permian extinction event in Vyazniki region, European Russia. Palaeogeogr. Palaeoclimat. Palaeoecol. *450*, 77–90.
17. Zaton, M., Broda, K., Qvarnström, M., Niedzwiedzki, G., and Ahlberg, P.E. (2017). The first direct evidence of a Late Devonian coelacanth fish feeding on conodont animals. Naturwissenschaften *104*, 26.
18. Barrios-de Pedro, S., Poyato-Ariza, F.J., Moratalla, J.J., and Buscalioni, Á.D. (2018). Exceptional coprolite association from the Early Cretaceous continental Lagerstätte of Las Hoyas, Cuenca, Spain. PLoS ONE *13*, e0196982.
19. Qvarnström, M., Wernström, J.V., Piechowski, R., Tałanda, M., Ahlberg, P.E., and Niedzwiedzki, G. (2019). Beetle-bearing coprolites possibly reveal the diet of a Late Triassic dinosauriform. R. Soc. Open Sci. *6*, 181042.
20. Qvarnström, M., Ahlberg, P.E., and Niedzwiedzki, G. (2019). Tyrannosaurid-like osteophagy by a Triassic archosaur. Sci. Rep. *9*, 925.
21. Qvarnström, M., Elgh, E., Owocki, K., Ahlberg, P.E., and Niedzwiedzki, G. (2019). Filter feeding in Late Jurassic pterosaurs supported by coprolite contents. PeerJ *7*, e7375.
22. Northwood, C. (2005). Early Triassic coprolites from Australia and their palaeobiological significance. Palaeontology *48*, 49–68.
23. Dzik, J., and Sulej, T. (2007). A review of the early Late Triassic Krasiejów biota from Silesia, Poland. Palaeontol. Pol. *64*, 3–27.
24. Qvarnström, M., Niedzwiedzki, G., Tafforeau, P., Žigaitė, Ž., and Ahlberg, P.E. (2017). Synchrotron phase-contrast microtomography of coprolites generates novel palaeobiological data. Sci. Rep. *7*, 2723.
25. Bethoux, O. (2009). The earliest beetle identified. J. Paleontol. *83*, 931–937.
26. Kukalová-Peck, J., and Beutel, R.G. (2012). Is the Carboniferous †*Adiphlebia lacoana* really the "oldest beetle"? Critical reassessment and description of a new Permian beetle family. Eur. J. Entomol. *109*, 633–645.
27. Fikácek, M., Beutel, R.G., Cai, C., Lawrence, J.F., Newton, A.F., Solodovnikov, A., Ślipinski, A., Thayer, M.K., and Yamamoto, S. (2020). Reliable placement of beetle fossils via phylogenetic analyses – Triassic *Leehermania* as a case study (Staphylinidae or Myxophaga?). Syst. Entomol. *45*, 175–187.
28. Beutel, R.G., and Haas, F. (2000). Phylogenetic relationships of the suborders of Coleoptera (Insecta). Cladistics *16*, 103–141.
29. Jałoszynski, P., Luo, X.-Z., Hammel, J.U., Yamamoto, S., and Beutel, R.G. (2020). The mid-Cretaceous †*Lepiceratus* gen. nov. and the evolution of the relict beetle family Lepiceridae (Insecta: Coleoptera: Myxophaga). J. Syst. Palaeontology *18*, 1127–1140.
30. Lamboy, M., Rao, V.P., Ahmed, E., and Azzouzi, N. (1994). Nanostructure and significance of fish coprolites in phosphorites. Mar. Geol. *120*, 373–383.
31. Hollocher, K.T., and Hollocher, T.C. (2012). Early processes in the fossilization of terrestrial feces to coprolites, and microstructure preservation. In Vertebrate Coprolites: New Mexico Museum of Natural History and Science Bulletin 57, A.P. Hunt, J. Milàn, S.G. Lucas, and J.A. Spielmann, eds. (New Mexico Museum of Natural History), pp. 79–92.
32. Chin, K., and Gill, B.D. (1996). Dinosaurs, dung beetles, and conifers; participants in a Cretaceous food web. Palaios *11*, 280–285.
33. Fikácek, M., Hu, F.-S., Aston, P., Jia, F.-L., Liang, W.-R., Liu, H.-C., and Minoshima, Y.N. (2020). Comparative morphology of immature stages and adults of *Hydroscapha* from Taiwan, with description of a new species from Hong Kong (Coleoptera: Myxophaga: Hydroscaphidae). Raffles Bull. Zool. *68*, 334–349.

34. Gordon, C.M., Roach, B.T., Parker, W.G., and Briggs, D.E.G. (2020). Distinguishing regurgitalites and coprolites: a case study using a Triassic bromalite with soft tissue of the pseudosuchian archosaur *Revueltosaurus*. Palaios *35*, 111–121.

35. Goloboff, P.A., Farris, J.S., and Nixon, K.C. (2008). TNT, a free program for phylogenetic analysis. Cladistics *24*, 774–786.

36. Ronquist, F., Teslenko, M., van der Mark, P., Ayres, D.L., Darling, A., Höhna, S., Larget, B., Liu, L., Suchard, M.A., and Huelsenbeck, J.P. (2012). MrBayes 3.2: efficient Bayesian phylogenetic inference and model choice across a large model space. Syst. Biol. *61*, 539–542.

37. Paganin, D., Mayo, S.C., Gureyev, T.E., Miller, P.R., and Wilkins, S.W. (2002). Simultaneous phase and amplitude extraction from a single defocused image of a homogeneous object. J. Microsc. *206*, 33–40.

38. Sanchez, S., Ahlberg, P.E., Trinajstic, K.M., Mirone, A., and Tafforeau, P. (2012). Three-dimensional synchrotron virtual paleohistology: a new insight into the world of fossil bone microstructures. Microsc. Microanal. *18*, 1095–1105.

39. Lyckegaard, A., Johnson, G., and Tafforeau, P. (2011). Correction of ring artifacts in X-ray tomographic images. Int. J. Tomogr. Simul. *18*, 1–9.

40. Lawrence, J.F., Ślipinski, A., Seago, A.E., Thayer, M.K., Newton, A.F., and Marvaldi, A.E. (2011). Phylogeny of the Coleoptera based on morphological characters of adults and larvae. Ann. Zool. *61*, 1–217.

41. Yavorskaya, M.I., Anton, E., Jałoszynski, P., Polilov, A., and Beutel, R.G. (2018). Cephalic anatomy of Sphaeriusidae and a morphology-based phylogeny of the suborder Myxophaga (Coleoptera). Syst. Entomol. *43*, 777–797.

42. Lewis, P.O. (2001). A likelihood approach to estimating phylogeny from discrete morphological character data. Syst. Biol. *50*, 913–925.

43. Rambaut, A., Drummond, A.J., Xie, D., Baele, G., and Suchard, M.A. (2018). Posterior summarization in Bayesian phylogenetics using tracer 1.7. Syst. Biol. *67*, 901–904.

44. Dzik, J., and Sulej, T. (2016). An early Late Triassic long-necked reptile with a bony pectoral shield and gracile appendages. Acta Palaeontol. Pol. *61*, 805–823.

45. Lucas, S.G. (1998). Global Triassic tetrapod biostratigraphy and biochronology. Palaeogeogr. Palaeoclimat. Paleoecol. *143*, 347–384.

46. Zaton, M., Piechota, A., and Sienkiewicz, E. (2005). Late Triassic charophytes around the bone-bearing bed at Krasiejów (SW Poland) – palaeoecological and environmental remarks. Acta Geol. Pol. *55*, 283–293.

47. Olempska, E. (2004). Late Triassic spinicaudatan crustaceans from southwestern Poland. Acta Palaeontol. Pol. *49*, 429–442.

48. Butler, R.J., Rauhut, O.W.M., Stocker, M.R., and Bronowicz, R. (2014). Redescription of the phytosaurs *Paleorhinus* ("*Francosuchus*") *angustifrons* and *Ebrachosuchus neukami* from Germany, with implications for Late Triassic biochronology. Zool. J. Linn. Soc. *170*, 155–208.

49. Pacyna, G. (2014). Plant remains from the Polish Triassic. Present knowledge and future prospects. Acta Palaeobot. *54*, 3–33.

## STAR★METHODS

### KEY RESOURCES TABLE

| REAGENT or RESOURCE | SOURCE | IDENTIFIER |
|---|---|---|
| Deposited data | | |
| Raw image data and 3D reconstructions | This paper | ESRF's database: http://paleo.esrf.eu/ |
| Software and algorithms | | |
| VGStudio MAX version 3.4.4 | Volume Graphics | https://www.volumegraphics.com/en/products/vgstudio-max.html |
| TNT | Goloboff et al.[35] | http://www.lillo.org.ar/phylogeny/tnt/ |
| MrBayes 3.2.6 | Ronquist et al.[36] | https://nbisweden.github.io/MrBayes/download.html |
| R | R Foundation for Statistical Computing | https://www.R-project.org/ |
| RStudio | RStudio | https://www.rstudio.com/ |

### RESOURCE AVAILABILITY

#### Lead contact

Further information and requests for resources should be directed to and will be fulfilled by the lead contact, Martin Qvarnström (martin.qvarnstrom@ebc.uu.se).

#### Materials availability

Coprolite ZPAL AbIII/3520 is stored at the Institute of Paleobiology, Polish Academy of Sciences (Warsaw).

#### Data and code availability

The reconstructed image stack from the synchrotron-scanned coprolite, models of the 15 type specimens, and figures derived from these models used for characters interpretation are publicly available in ESRF's database: http://paleo.esrf.eu/. The publication is registered in ZooBank: http://zoobank.org/urn:lsid:zoobank.org:pub:6FB8E4B4-51C6-493C-A1E6-1829B9258993 for the purpose of the zoological nomenclature. The newly proposed names are registered under the following doi numbers: Triamyxidae – Zoobank: http://zoobank.org/urn:lsid:zoobank.org:act:A917002F-D2AA-4F13-A5E6-ABA9B5F57FC2; *Triamyxa* – *Zoobank:* http://zoobank.org/urn:lsid:zoobank.org:act:4BAE2CFB-A798-4465-A9BF-5D118E552861;*Triamyxa coprolithica* – Zoobank: http://zoobank.org/urn:lsid:zoobank.org:act:41F68910-6C91-4DE5-8A21-38EBD96C1E97.

### EXPERIMENTAL MODEL AND SUBJECT DETAILS

The studied coprolite specimen ZPAL AbIII/3520 is stored at the Institute of Paleobiology, Polish Academy of Sciences (Warsaw). The holotype (Figures 1B–1D) and paratypes (Figures 1E–1G and 1I) of the myxophagan beetle *Triamyxa coprolithica* gen. et sp. nov. are preserved as inclusions within this coprolite fragment, and the imaging of these were done using synchrotron microtomography.

### METHOD DETAILS

#### Synchrotron microtomography

The coprolite fragment was scanned at the European Synchrotron Radiation Facility (ESRF) in Grenoble, France, as a part of project ES145. The coprolite was mounted in a tube that was scanned in vertical series of 4 mm in half-acquisition mode, i.e., the center of rotation was set at the side of the camera field of view resulting in a twofold increase of the field of view. The distance between the sample and the camera (propagation distance) was 2800 mm. The camera was a sCMOS PCO edge 5.5 detector, mounted on optical devices bringing an isotropic voxel size of 6.36 μm, and coupled to a 500-μm thick LuAG:Ce (lutetium aluminum garnet doped with cerium) scintillator. The beam was produced by a W150 wiggler (11 dipoles, 150 mm period) with a gap of 51 mm and was filtered with 2.8 mm aluminum and 6 mm copper. The resulting detected spectrum had an average energy of 112 keV. Each sub scan was performed using 6000 projections of 0.05 s over 360 degrees. The reconstructions of the scan data were done using a phase retrieval approach.[37,38] Ring artifacts were corrected using an in-house correction tool.[39] The final volumes consist in stacks of 16 bits TIFF images that were converted into JPEG2000 images and subsequently imported and segmented in the software VGStudio MAX version 3.0 (Volume Graphics).

## Examined material and character reconstruction

For character coding, we analyzed 15 beetle specimens found in ZPAL AbIII/3520 (Figure 1): complete beetles with appendages (2 specimens), near-complete beetles with legs, elytra or head missing (7 specimens), isolated prothorax and head (1 specimen), isolated meso- and metaventrite (1 specimen), isolated pronotum (3 specimens), and isolated head (1 specimen). All these specimens share details of morphology and are most likely conspecific. In addition, we measured 55 isolated elytra from the coprolite (Figures S1 and S2). Borders between sclerites of the body (pronotum versus elytra in dorsal view, sutures of pro- meso- and metathorax in ventral view) are not recognizable in complete beetles but can be visualized using disarticulated body parts; these parts were superimposed on complete specimens in order to obtain a reconstruction of the beetle as complete as possible. Some structures (e.g., segmentation of antenna and tarsi) are difficult to interpret precisely; these structures are marked in red in the reconstruction (Figure 3) and are not coded in matrices used for phylogenetic analyses.

## Phylogenetic analyses

Two sets of analyses were done, the first testing the position of the beetle in the entire order Coleoptera, and the second testing its position in the suborder Myxophaga (Figure S2). For the former analyses we coded the preserved characters into the data matrix provided by Lawrence et al.[40] This dataset includes 359 terminal taxa covering all extant families and seven holometabolan outgroups; 344 adult characters were coded for each taxon. We were able to code 77 characters for the fossil beetle (i.e., 22.3% of adult characters). For analyses focused on Myxophaga, we used the matrix of Yavorskaya et al.[41] containing 58 adult and 38 larval characters and two characters concerning biology. We coded 17 characters for the fossil beetle (i.e., 17.5% of characters). In the analyses, we followed the approach of Fikácek et al.,[27] which allows the fossil to move freely across the topology of modern taxa fixed according to recent molecular studies; we used the same topology constraints as in Fikácek et al.[27] Maximum parsimony analyses were performed in TNT[35] using exhaustive search for topology-constrained analyses and Traditional Search with 1000 replicates and 100 trees saved per replicate for unconstrained ones. Bayesian analyses were carried out in MrBayes 3.2.6,[36] with the *Mk* model for morphology[42] corrected only for variable characters scored, equal state frequencies and gamma-distributed rate variation across characters. The molecular topology of modern taxa was imposed as a set of partial topology constraints. Since the prothoracic morphology excluded the position of the fossil in Polyphaga, an additional analysis with a hard constraint imposing the monophyly of this suborder (excl. the fossil) was carried out. The analyses were run for 10 million (Coleoptera analyses) or 5 million generations (Myxophaga analyses) with two runs, each with one cold and three heated chains. Output of all analyses was inspected in Tracer 1.7[43] for parameters of convergence and effective sample size. Consensus trees were constructed with 25% burn-in. The uncertainty of the placement of the fossil beetle in the final Bayesian consensus tree, its alternative placements and their posterior probabilities were visualized using an R script from Fikácek et al.[27] Results of the analyses of the placement of *Triamyxa* in the Myxophaga dataset is presented in Figure S3.

## Characters coded for Coleoptera analysis

(character states coded from 0, in difference to Lawrence et al.[40] where they are coded from 1)

77 characters coded

1. Head: (0) not completely concealed from above by pronotum.
2. Head at base: (0) declined less than 45 degrees.
3. Head behind eyes: (0) not or gradually constricted laterally, without temples.
11. Vertex: (0) not or slightly declined.
13. Eyes: (0) at least slightly protuberant, extending laterally beyond sides of head as seen from above.
14. Eyes: (0) undivided.
15. Vertical eye diameter: (0) less than 1.25 times greatest horizontal eye diameter.
20. Antennal socket: (0) not located within eye emargination.
22. Antennal sockets: (0) not completely concealed by frontal ridges, at least partly visible in dorsal or frontal view
23. Antennal sockets separated by: (1) at least 1.5 times diameter of socket.
26. Frontoclypeal region at midline: (0) not or only slightly, gradually declined.
30. Clypeus: (0) not subdivided.
31. Length of muzzle or rostrum: (0) less than width of clypeus or frontoclypeus.
35. Labral apex: (2) truncate.
38. Antennal flagellum: (3) capitate, with one or more apical antennomeres distinctly wider and/or longer than preceding ones.
40. Antenna: (0) not geniculate or elbowed, pedicel not forming angle with scape.
41. Antennal scape: (1) 1 to 3 times as long as pedicel.
43. Scape: (0) parallel-sided or only slightly curved.
44. Pedicel: (0) not partly enclosed within scape.
47. Antennal club: (0) not 5-segmented or with second club segment subequal to or larger than first one.
49. Antennal club: (0) not or only slightly asymmetrical.
53. Mandible: (0) visible in lateral view.
72. Maxillary palps: (0) elongate, projecting anterolaterally, usually extending well beyond apex of galea.

74. Apical maxillary palpomere: (0) not or only slightly shorter or narrower than preapical palpomere.
82. Mentum or postmentum: (0) widest at or near base.
84. Mentum: (0) not enclosed by lateral lobes of submentum.
85. Mentum: (0) separated from submentum or gulamentum by suture.
95. Sides of prothorax: (0) not explanate.
96. Sides of prothorax: (0) with complete lateral carinae separating disc from hypomeron on each side.
100. Edge of lateral pronotal carina: (0) simple or minutely crenulate.
102. Anterior pronotal angles as viewed from above: (1) produced forward and broadly rounded, or (2) produced forward and narrowly rounded, or (3) produced forward and acute.
105. Posterior edge of pronotum: (1) distinctly sinuate, angulate or variously lobed.
107. Pronotal disc: (0) without sublateral carinae.
108. Posterior, sub-basal portion of pronotal disc: (0) without paired impressions.
109. Mesolateral portions of pronotum: (0) without deep pits formed by internal apodemes.
110. Ventral or lateral portion of prothorax on each side: (0) with notopleural and pleurosternal sutures (notum and sternum completely separated by pleuron), or (1) with notosternal, pleurosternal and notopleural sutures (notum and sternum abutting anteriorly).
114. Procoxal cavities: (1) well developed, procoxae distinctly countersunk.
117. Lateral portion of prosternum in front of middle of procoxal cavity or procoxal base: (1) 0.5 to 2 times as long as mid length of cavity or coxal base at that point.
119. Prosternal ''chin-piece'': (0) absent.
120. Anterior edge of prosternum: (0) not abruptly excavate at middle.
121. Prosternal process: (2) incomplete, ending before posterior edge of coxa, or absent.
122. Portion of prosternal process extending behind coxae: (0) absent.
124. Prosternal process in ventral view: (0) not expanded apically.
137. Procoxal cavities externally: (0) broadly open.
138. Procoxal cavities internally: (2) broadly closed.
139. Procoxal cavities: (0) contiguous or separated by less than 0.25 times shortest diameter of coxal cavity.
141. Postcoxal projections of propleuron or pronotal hypomeron: (0) absent or very short and usually rounded, angulate or truncate.
149. Elytral apices: (1) meeting at midline, squarely or obliquely truncate.
150. Elytra: (0) concealing all abdominal tergites or exposing part of one only.
152. Elytra: (0) without window punctures.
163. Anterior edge of mesoventrite at midline: (1) on different plane than metaventrite.
169. Mesoventral cavity for reception of prosternal process: (0) absent.
172. Mesoventral process: (0) extending to or beyond anterior edge of metaventrite.
173. Apex of mesoventral process: (2) undivided, broadly rounded or truncate.
174. Mesocoxae: (0) not strongly projecting.
178. Mesocoxal cavities: (1) moderately deep, and completely demarcated mesally and posteriorly by sharp ridge.
179. Mesocoxal cavities: (0) circular to slightly transverse and not or only slightly oblique.
180. Mesocoxal cavities: (2) separated by more than 0.75 times shortest diameter of coxal cavity.
181. Mesocoxal cavity bordered by: (6) mesoventrite and metaventrite.
183. Internal portions of mesothorax and metathorax: (1) separated from one another by suture or line, or (2) solidly fused, without suture.
184. Mesoventral and metaventral processes: (6) solidly fused together but separated by suture or line.
185. Mesometaventral junction at midline: (0) exposed or absent.
190. Exposed portion of metanepisternum: (1) 2.5 to 5.0 times as long as its greatest width.
193. Angle formed at midline by horizontal line and line tangential to anterior edge of metacoxa: (1) at least 30 degrees.
194. Metacoxa: (0) not longer at middle than adjacent portion of metaventrite.
195. Transverse extent of metacoxa: (2) more than 3 times as long as longitudinal extent.
196. Metacoxae: (0) contiguous or separated by less than 0.2 times transverse diameter of one coxa.
198. Metacoxae: (0) more or less movable.
199. Metacoxae mesally: (0) completely free from one another.
200. Metacoxal plates: (1) well developed mesally but weakly developed or absent laterally.
201. Metacoxal plates: (0) concealing no ventrites.
250. Mesotibia: (0) not strongly widened.
268. Abdominal ventrites in male: (6) six or (7) five.
269. Basal abdominal ventrites connate: (0) none.
270. Abdominal ventrite one: (0) on same plane as ventrites two and three.

276. Ventrite 1 at about midpoint between midline and lateral edge of abdomen: (2) 1.0 to 1.5 times as long as ventrite 2 at same point.
277. Basal abdominal ventrite (0) continuous across base of abdomen.
287. Tergite VII and sternite VII: (0) separated by membrane or a distinct suture.

### Characters coded for Myxophaga dataset

17 characters coded

1. Head shape: (1) elongate, conical, peristome present.
7. Distal part of scapus and pedicellus: (0) not urn-shaped.
12. Enlarged terminal antennomere: (0) absent.
14. Exposure of paired mouthparts: (0) largely or completely visible externally.
19. Size of penultimate maxillary palpomere: (0) not distinctly larger than preceding palpomeres.
20. Apical maxillary palpomere: (0) not distinctly smaller than preceding palpomeres.
22. Connection of mentum and submentum: (0) separate.
30. Width of prosternal process: (0) narrow or moderately wide.
31. Apex of prosternal process: (0) not truncated.
32. Exposure of propleuron: (0) free.
34. Connection of pterothoracic ventrites: (1) firmly connected.
35. Separation of mesocoxae: (1) widely separated.
37. Elytral apex: (1) truncated.
40. Separation of metacoxae: (0) medially adjacent or narrowly separated.
41. Metacoxal plates: (2) broad and concave posteriorly.
48. Shape of abdominal segments V–VIII: (0) not narrowed and ring-like.
49. Exposure of ventrite 2 (sternite IV): (0) not covered by ventrite 1.

### Results of phylogenetic analyses (see also Figures S2 and S3)

#### *Coleoptera dataset – constrained topology with fossil free to move*

- Bayesian, without Polyphaga constrained: *Triamyxa* as stem group of Staphylonoidea (with moderate pp = 0.67), alternative placements are in Staphyliniformia (most supported is Ptiliidae: *Actrotrichis*, and Staphylinidae: Scaphidiinae: *Scaphidium*) and Cucujiformia (with very low pp).
- Bayesian, with Polyphaga constrained: With Polyphaga kept monophyletic (following the prothorax mophology which clearly had notopleural suture and exposed propleuron): *Triamyxa* sister to all extant Myxophaga (high pp = 0.95). In maximum credibility consensus tree placed as sister to all modern Myxophagan families.

#### *Myxophaga dataset, maximum parsimony*

- Unconstrained without *Leehermania*: sister to Hydroscaphidae
- Unconstrained with *Leehermania*: in polytomy with Sphaeriusidae, modern Hydroscaphidae, *Leehermania* and Torridincolidae.
- Constrained with and without *Leehermania*: basal polytomy with Hydroscaphidae and (Sphaeriusidae+Lepiceridae+Torridincolidae)

#### *Myxophaga dataset, Bayesian analyses*

- Unconstrained: basal polytomy with Lepiceridae and (Hydroscaphidae+Sphaeriusidae+Torridincolidae)
- Constrained: sister to all modern Myxophaga

### Description of Triamyxa coprolithica gen. & sp. nov

Body length 1.4–1.7 mm, elytra 0.9–1.3 mm long and 0.4–0.5 mm wide. Body elongate, navicular, slightly compressed dorsolaterally. Head. ca. as long as wide, gradually narrowing behind eyes, strongly narrowed and slightly prolonged in front of eyes. Anterior margin of head (?labrum) subquadrate. Genal folds not developed, and hence mandibles visible laterally. Compound eyes large, strongly protruding laterally. Mentum transverse, with its posterior margin reaching slightly anteriad of mid-length of eyes, anterior margins weakly rounded. Maxillary stipes elongate. Maxillary palpi elongate; penultimate maxillary palpomere slender, slightly shorter than terminal one; terminal palpomere long and slender, fusiform. Antennae inserted dorsally in a depressed area of frons between eyes; scapus large, elongate, pedicel shorter; apical portion of antenna with slightly enlarged antennomeres, apparently forming a slightly widened antennal club. Number of antennomeres uncertain, but probably 9 as suggested by available reconstructions: scape, pedicel, 4 intermediate antennomeres and 3 antennomeres of the antennal club. Prothorax. Pronotum strongly narrowing

anteriad, anterolateral corners strongly projecting; posterolateral corners subacute; posterior margin strongly projecting posteriad, likely covering scutellar shield; dorsal disc evenly arcuate, without distinct grooves or ridges; ventral hypomeral portion of pronotum separated from dorsal disc by distinct edge, rather narrow, posteromesally projecting as a small tooth. Prosternum in front of procoxae long, anteriorly possibly in narrow contact with pronotum; its mesal portion slightly raised; posteromesally projecting as very short and rounded prosternal process. Propleuron present and exposed, drop-shaped (it may or may not reach anterior margin of prothorax, reconstruction of this region is ambiguous). Procoxal cavities closed internally and widely open externally along entire posterior margin. Mesothorax slightly shorter than metathorax on ventral side. Mesoventrite with wide subpentagonal elevation posteriorly broadly meeting metaventrite; laterally bordering anterior margin of very widely separated mesocoxal cavities; likely at least partly separated from mesanepisternum, wide anteriorly, with anapleural sutures slightly diverging posteriorly. Mesocoxal cavities rounded, very widely separated from each other, completely bordered by meso- and metaventrite. Elytra long, dorsally covering complete abdomen except for last one or two segments (see below); elytral apex truncate; elytral epipleura likely reaching level of metathorax. *Metathorax* wider than long on ventral side, anteromesally with a wide projection meeting mesoventral elevation. Metanepisternum moderately wide. Metacocal cavities transverse, reaching lateral border of metaventrite but not elytral epipleura. *Abdomen* with 5–6 exposed ventrites (since specimens with both 5 and 6 ventrites are present in the material examined, we conclude that either the 6$^{th}$ ventrite is highly movable and may be either totally retracted or largely protracted, or alternatively that the morphology of the abdomen is sexually dimorphic, with females with 5 ventrites and males with 6 ventrites). Ventrite very long, extensive, with narrow intercoxal projection; ventrite 2 slightly more than half as long as 1, 3 slightly shorter than 2, and 4 slightly shorter than 3; ventrite 5 parabolic, with evenly rounded posterior margin; ventrite 6 (if present) narrow and very elongate; all segments with tergites separated from sternites by lateral membrane, no abdominal segment entire and conical. One specimen with 6 ventrites apparently displays a slightly protruding, narrow rod-like aedeagus. *Legs.* Pro- and mesocoxa subglobular; metaxoca transverse, with narrow plates partly covering metafemora and basal portion of proximal abdominal ventrite. Trochanters of all legs small. Femora narrow and elongate, with tips reaching or slightly overtopping body outline; mesofemur narrow basally, widened distally. Tibiae slender, slightly bent inward. Tarsi short, very likely with relatively long terminal tarsomere, but subdivision and number of tarsomeres not clearly preserved; all tarsi with a pair of massive claws.

### The locality

The Upper Triassic section at Krasiejów in Poland presents an almost 30-m thick succession with variegated mudstones and thin lenses of calcareous grainstones. Two main fossil-bearing intervals comprise remains of both lacustrine and terrestrial.[23] The latter consists of a large predatory rauisuchian (*Polonosuchus silesiacus*), an aetosaur (*Stagonolepis olenkae*), a dinosauriform (*Silesaurus opolensis*), an archosauromorph (*Ozimek volans*), and various small other diapsids.[23,44] The freshwater fauna includes temnospondyls (*Metoposaurus krasiejovensis* and *Cyclotosaurus intermedius*), a large phytosaur (*Parasuchus* sp.), actinopterygians, a hybodont (*Lonchidion* sp.) and various invertebrates.[23,44] A late Carnian age of the fossil assemblage is inferred from plant macrofossils, the vertebrate community, conchostracans, and charophytes,[23,45–49] since there are no radiometric dates from the succession.

## QUANTIFICATION AND STATISTICAL ANALYSIS

The statistical analyses, which are described in detail under Method Details, were performed using TNT[35] and MrBayes 3.2.6.,[36] the summary of results was prepared in R (R Foundation for Statistical Computing) and RStudio (RStudio).

## ADDITIONAL RESOURCES

Reconstructed images, 3D reconstructions, and associated data from the synchrotron scanning are publicly available in the ESRF heritage database for palaeontology, evolutionary biology and archaeology: http://paleo.esrf.eu/.

**Current Biology, Volume *31***

## Supplemental Information

# Exceptionally preserved beetles in a Triassic coprolite of putative dinosauriform origin

**Martin Qvarnström, Martin Fikáček, Joel Vikberg Wernström, Sigrid Huld, Rolf G. Beutel, Emmanuel Arriaga-Varela, Per E. Ahlberg, and Grzegorz Niedźwiedzki**

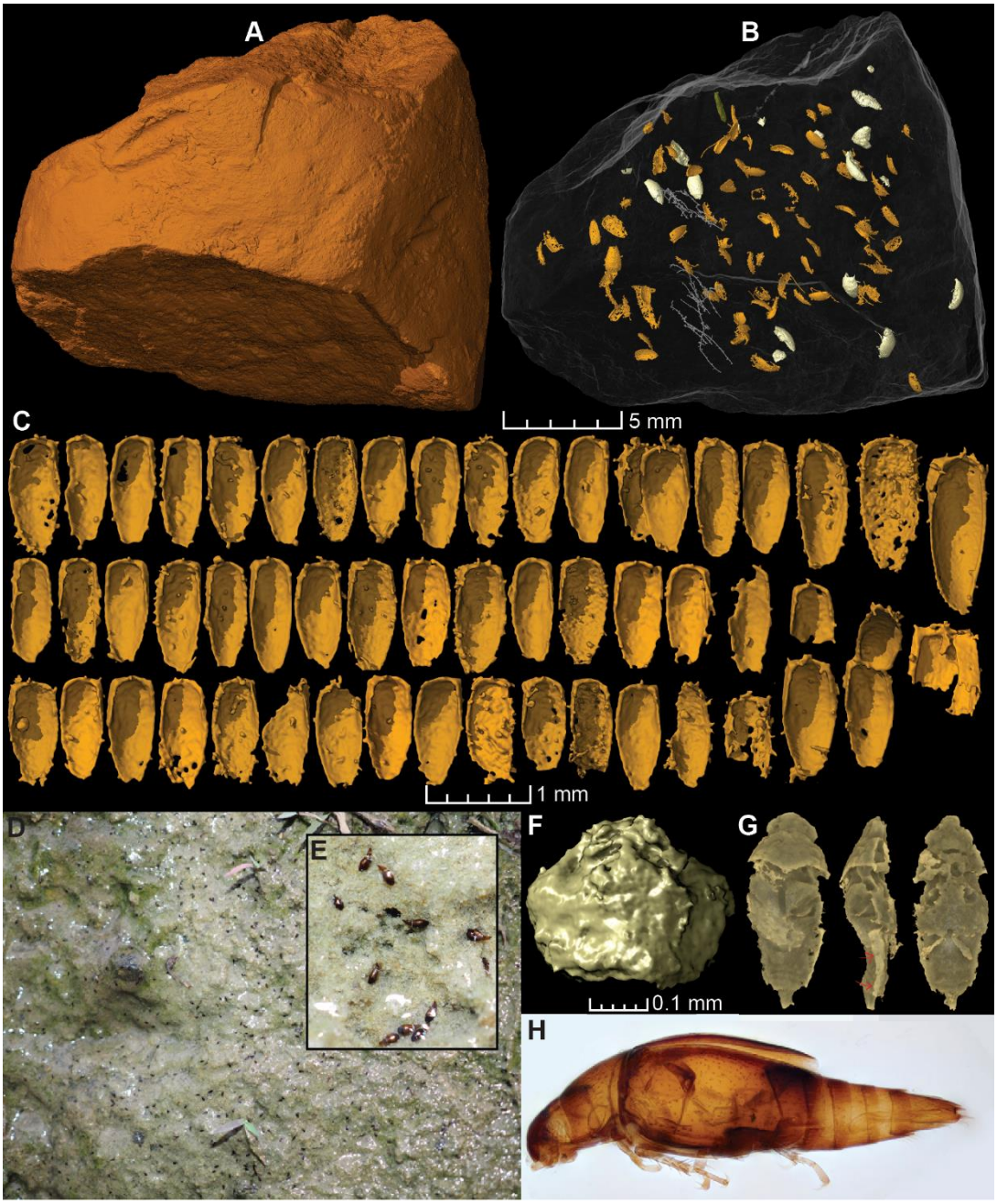


**Figure S1. Coprolite contents and comparisons of *Triamyxa* with recent myxophagans, related to Figure 1 and STAR Methods. A–B:** the coprolite rendered in 3D (A) and in semi-transparent with visible inclusions (B). **C:** ventral views of 3D-reconstructed elytra from the coprolite. **D–E:** mass occurrence of modern myxophagan beetles in algal mats: example of *Hydroscapha takahashii* in Taiwan (photos by F.-S. Hu, with permission). **F:** detail of the isolated head of *Triamyxa coprolothica* gen. & sp. nov. in ventral view. **G:** reconstruction of *Triamyxa coprolithica* gen. & sp. nov., specimen 4; lateral view shows the dorsoventrally compressed abdomen with a lateral 'ridge' typical for beetle groups in which tergites and sternites are well defined and laterally separated by a membranous pleural region. In contrast, in groups with fused tergites and sternites (incl. myxophagan Hydroscaphidae), the abdominal segments are always conical in shape, without dorsoventral compression and the lateral 'ridge'. **H:** lateral view of a KOH-treated specimen of *Hydroscapha takahashii*; note the absence of any 'ridge' at the lateral side of the abdomen, caused by the lateral fusion of tergites and sternites, resulting in ring-like abdominal segments. Even in specimens strongly treated with KOH (and hence with softened cuticle), the abdomen never collapses dorsoventrally to the form present in *Triamyxa*.

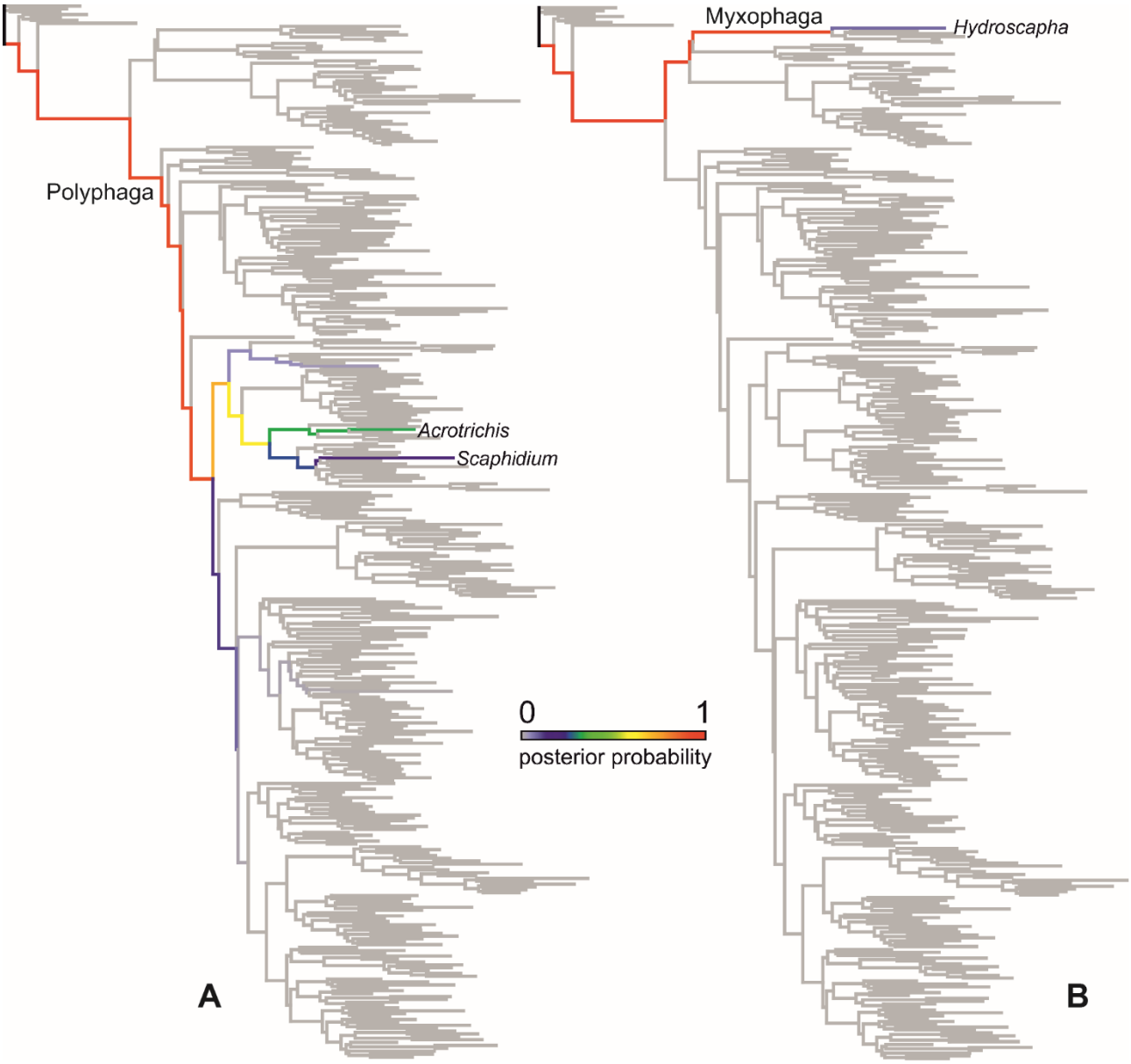


**Figure S2**. **Analysis of alternative placements of *Triamyxa* in the Bayesian analysis of Coleoptera dataset, related to Figure 3 and STAR Methods. A:** unconstrained analysis in which a moderately supported placement of *Triamyxa* in Staphylinoidea is revealed (orange and yellow branches), with weakly supported family placements in Ptiliidae (*Actrotrichis*), Staphylinidae: Scaphidiinae (*Scaphidium*). **B:** constrained analysis with imposed monophyly of Polyphaga, in which a single highly supported placement in Myxophaga is revealed.

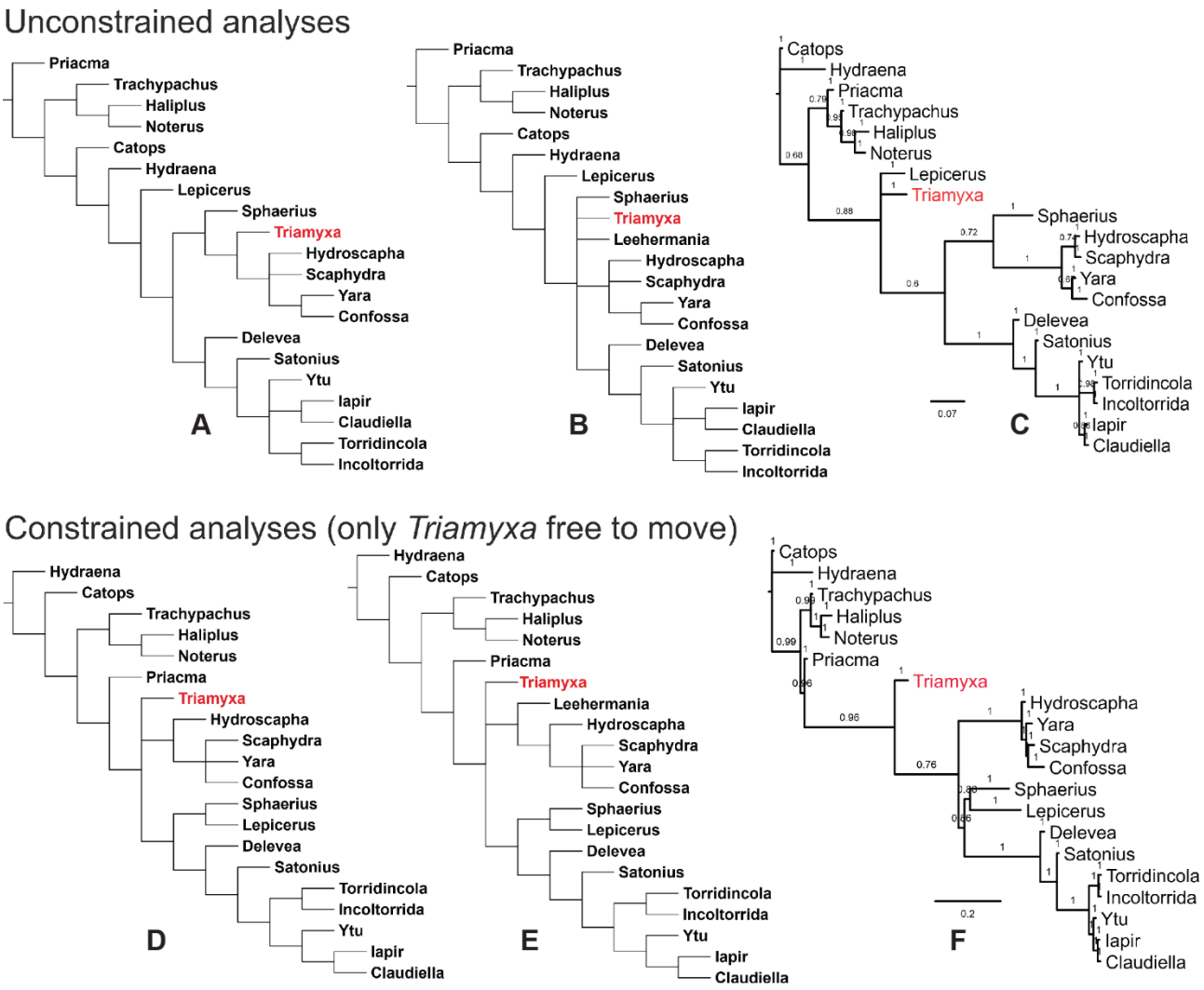


**Figure S3. Results of the analyses of the placement of *Triamyxa* in the Myxophaga dataset, related to Figure 3 and STAR Methods. A–C:** unconstrained analyses. **D–F:** analyses with the position of recent taxa fixed according to recent molecular analyses, and the position of *Leehermania* (in B and E) according to the analysis by Fikáček et al.[36]; only *Triamyxa* is free to move. Analyses: A, D – maximum parsimony analysis with modern taxa plus *Triamyxa*; B, E – maximum parsimony analysis with modern taxa plus Leehermania plus *Triamyxa*; C, F – Bayesian analysis with modern taxa plus *Triamyxa*.

| | **Triamyxidae fam. nov.** | **Hydroscaphidae: *Leehermania*** | **Hydroscaphidae: modern** | **Sphaeriusidae** | **Torridincolidae** | **Lepiceridae** |
|---|---|---|---|---|---|---|
| Dorsal surface | smooth | smooth | Smooth or sculptured | smooth | smooth or sculptured | tuberculate |
| Head anteriorly of eyes | long and narrowed | short, slightly narrowed | short to moderately long, at most slightly narrowed | short, rounded | long and narrowed | long, not narrowed |
| Genal folds (mandibles) | absent (m. visible laterally) | present (m. concealed) | present (m. concealed) | present (m. concealed) | present (m. concealed) | present (m. concealed) |
| Eyes | strongly protruding | not protruding | not protruding or slightly protruding (*Confossa*) | not protruding | weakly to strongly protruding | strogly protruding |
| Antennal bases | exposed, dorsally between eyes | concealed dorsally, anterior of eyes | concealed dorsally, anteriorly of eyes | exposed, dorsally between eyes | exposed, dorsally anterior or between eyes | concealed dorsally, anterior of eyes |
| Antennomeres | probably 9 | 11 | 9 or 5 (*Scaphydra*) | 11 | 9 or 11 (*Develea*) | 5-7 |
| Scapus + pedicel | separated, exposed externally | separated, scapus exposed | separated, scapus concealed | separated, exposed externally | closely attached | separated, scapus concealed |
| Antennal club | present (probably of 3 antennomeres) | present (of 3 antennomeres) | terminal antennomere widened | present (of 3–4 antennomeres) | absent (but whole antenna club-like) | terminal antennomere widened |
| Terminal maxillary palpomere | long | minute | minute | minute | long | long |
| Mentum | large, narrowing anteriad | ? | tiny | large, narrowing anteriad | moderately large, expanding anteriad | large |
| Prosternum in front of procoxae | long | moderately long | short | very short | moderaly long | short |
| Prosternal process | wide and very short, blunt | short, pointed | short, pointed | absent | very wide | moderately long, pointed |
| Mesoventrite | slightly shorter than metaventrite | much shorter than metaventrite | much shorter than metaventrite | much shorter than metaventrite | much shorter than metaventrite | slightly shorter than mesoventrite |
| Mesoventral elevation | wide, subpentagonal | ? | narrow, subpentagonal | wide, subpentagonal | wide, subquadrangular (truncate anteriorly) | wide, subpentagonal |
| Anapleural sutures | at least partly present | ? | absent | absent | absent | absent |
| Elytra | long | short | short | long | long | long |
| Elytral apex | truncate | truncate | truncate | not truncate | not truncate | not truncate |
| Exposed abdominal segments dorsally | 1–2 | 4–5 | 4–5 | 0 | 0 | 0 |
| Metanepisternum anteriorly | moderately wide | moderately wide | moderately wide | absent | narrow | narrow |
| Metacoxal plates | narrow, narrowly separated | narrow, contiguous | narrow, contiguous to widely separated | large, contiguous | absent, metacoxae contiguous to narrowly separated | absent, metacoxae widely separated |
| Abdominal ventrites | 5–6 (likely 5 in female, 6 in male) | 6 | 6 | 3 | 4-5 | 5 |
| Abdominal segments III-VI | divided in tergite and sternite | conical, not subdivided | conical, not subdivided | divided in tergite and sternite | divided in tergite and sternite | divided in tergite and sternite |
| Tarsal formula | ? | ? | 3-3-3 | 3-3-3 | 5-5-5 or 4-4-4 | 1-1-1 |

**Table S1. Diagnosis and comparison of Triamyxidae with modern Myxophagan families and *Leehermania* (extinct Hydroscaphidae), related to STAR Methods.**